Applied Mathematics & Information Sciences
An International Journal

http://dx.doi.org/10.18576/amis/13S140

Liver Tumor Localization Using an Integrated Hybrid Fuzzy Seed Point Region Growing Algorithm

Shaimaa A. Elmorsy[1,*] , *Mohamed A.Abdou*[2] , *Yasser F.Hassan*[1] and *Ashraf Elsayed*[1,3]

[1] Faculty of Science, Alexandria University, Alexandria, Egypt.
[2] Informatics Research Institute, City of Scientific Research &Technological Applications, Alexandria, Egypt.
[3] University of Science and technology, Zewail City of Science and Technology, October Gardens, 6th of October, Giza, Egypt.

Received: 25 Apr. 2019, Revised: 17 Jun. 2019, Accepted: 1 Jul. 2019

Abstract: Image processing is one of the most important fields to replace non-invasive diagnosis in Hepatocellular Carcinoma (HCC). Liver segmentation is one of the main processes in the detection of many liver diseases non-invasively. Accurate liver tumor segmentation is of great importance in tumor detection and localization. This paper proposes an integrated hybrid fully automatic method for tumor segmentation for abdominal 2D CT scans together with the detection of tumor main parameter (size, percentage to the liver and safe area). The proposed FSPRG method uses the Fuzzy C-means method as a first step, followed by a complementary region-growing method that builds its knowledge on the Fuzzy C-means stage. After tumor segmentation process finishes the main parameters of tumor are calculated using Laplacian of Gaussian (LOG) curve. The whole process is applied to a set of 2D CT of primary diagnosed HCC patients and the proposed algorithm. Results show that the proposed integrated method succeeds in segmenting the tumor region from the liver.

Keywords: medical image processing, HCC, computed tomography, Fuzzy C-means, Region growing, Laplacian of Guassian.

1 Introduction

liver cancerous cells are that cells that grow in an abnormally and uncontrolled way. Liver cancer causes the liver not to function in a normal way which makes it one of the most life-threatening diseases in the world. Invasive techniques are the most wide world techniques that are used for accurate diagnosis for the disease avoiding the noninvasive techniques like biopsy that causes pain and medical complications for some patients [12]. Medical image processing is one of the most popular techniques that are used for accurate diagnosis of the disease. In medical image processing, the intensity similarity between the tissues in the abdominal Computed Tomography (CT) images is the most challenging problem in tumor segmentation process. This similarity problem makes the process of generating a fully automatic algorithm for tumor liver segmentation from 2D CT challenging and not that easy. There are many methods that have been used in many tumor segmentation techniques specially those of liver, one of these methods is the clustering-based method which is one of the famous grey-level-based methods [14].

Clustering is one of the most active research areas in the machine learning domain [22-25] and plays a significant role in many applications such as medical diagnosis. Generally, in clustering based methods the main concept is that given a space with n-dimension feature that is divided into classes and the members of the classes is determined according to the distance between them. If the distance between the samples of the space and the center of a specific class is shorter than the distance to the centers of the other classes then they belong to the same class. The samples of the same classes have higher similarity between each other than between members of other classes. Fuzzy C-Means (FCM) clustering and k-means clustering are generally the main two methods based on the clustering

---

[*] Corresponding author e-mail: shaimaa_elmorsy@hotmail.com

which is used on the segmentation of the liver [1]. As any clustering-based method [1,3], the Fuzzy FCM method has its own advantages and disadvantages. The main advantage is that it can manage the process of segmentation fully automatically without any need to any intervention. On the other hand, the results of FCM may contain many false positive regions due to the intensity similarity between the tissues of the liver and the lesions that aimed to be extracted. The need for post processing after applying the FCM is an imperative issue. The improvement of the results of the FCM method for segmentation has been an active field for the researchers in the past few years either by improving the FCM method itself or by integrating FCM and other methods for more accurate segmentation results. For example, in [4] the authors proposed a new fuzzy level set algorithm that used FCM method integrated with level set as initial function, the proposed algorithm proved the ability of boundary of interest approximation. A new extended FCM algorithm was innovated by the authors in [5] for image segmentation, where the results were also used as an initial parameters of level set contour and the results were promising. An approach of liver tumors detection and segmentation was proposed in [6], where the authors used FCM method as a second stage that will be used as an intermediate stage before the tumor final detection stage that used DRLSE (Distance Regularized Level Set Evolution) and the results proved the effectiveness of their approach. In [7] the authors proposed an integrated hybrid method which integrates cuckoo optimization and fuzzy c-means algorithm with random walkers algorithm. The proposed integration proved its effectiveness through the results.

This paper introduces a hybrid integrated approach for finding a completely automatic way for solving the problem of tumor liver's pixels acquisition from a segmented liver CT medical image and finding the parameters of the segmented tumor (height and width) together with predicting the safe area surrounding the tumor. The paper will be organized as follows: Section 2 introduces the proposed fuzzy seeded point region growing method (FSPRG). Section 3 represents the experimental results and dataset description that will be used. The paper will end up with a conclusion in section 4.

2 Proposed Fuzzy Seed Point Region Growing Method (FSPRG)

This subsection of the work first starts by reviewing the main methods that are used in the introduced algorithm. The main frame of fuzzy c-means algorithm that is used as the initial step of the proposed algorithm as a primary step for tumor segmentation is explained. The region-growing algorithm that is used in the proposed algorithm to improve the results of segmentation is explained. The framework of the proposed FSPRG method will be proposed with an illustrated example.

2.1 Fuzzy C-means Method

The main idea of FCM is the membership degree which is that every point in the space belongs to all defined classes with a specific membership degree other than belonging to a unique specific class[2,4]. The fuzzy C-means algorithm is explained in [3] as follows: The main aim of the Fuzzy C-means algorithm is to minimize the objective function (O_f) which is stated in equation (1).

$$O_f = \sum_{i=1}^{D} \sum_{j=1}^{N} \mu_{ij}^{m} \left\| x_i - c_j \right\|^2 \qquad (1)$$

where, D is the number of pixels of the image, N is the clusters number, m is a fuzzy partition matrix exponent for controlling the degree of fuzzy overlap, xi denotes the image pixel number i, c_j is the cluster number j and μ_{ij}^{m} is the degree of membership of point x_i in cluster c_j .

The fuzzy C Means algorithm clusters the input data by the following steps as shown in figure 1.

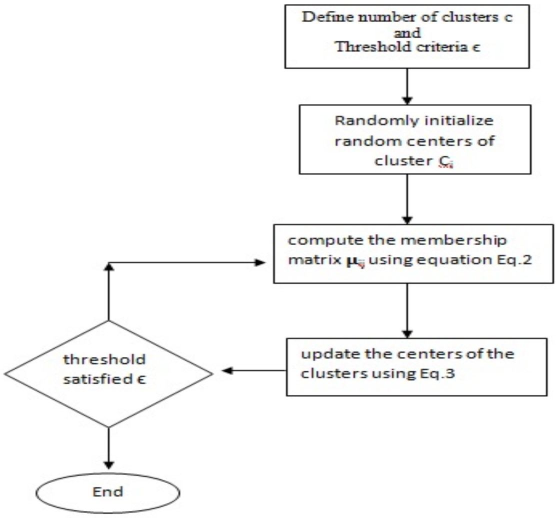

Fig. 1: Flow chart of fuzzy C-means Algorithm.

First: the initialization step, where an initial clusters centers are chosen, then the initial membership value is calculated for each pixel to determine the initial membership degree of each point in the input data to each cluster center using Eq. (2), finally, the initial objective function is calculated using Eq. (1). Second: After the initialization step the new centers will be calculated, the new membership values for each input is calculated for the new clusters using Eq. (3) which will leads to a new objective function value. Third: the new clusters is updated, the membership of each pixel is calculated with respect to the centers of the new clusters and the new objective function will be calculated using the updated information. The update step is repeated until the conversion satisfies the following conditions either the number of iterations is reached or the objective function (O_f) is improved less than a specific threshold.

$$\mu_{ij} = \frac{1}{\sum_{k=1}^{N} \left(\frac{\|x_j - c_i\|}{\|x_j - c_k\|} \right)^{\frac{2}{m-1}}} \quad (2)$$

$$c_j = \frac{\sum_{i=1}^{D} \mu_{ij}^{m} x_j}{\sum_{i=1}^{D} \mu_{ij}^{m}} \quad (3)$$

2.2 Region-Growing Method

The idea of region-growing means comparing the intensities of the neighboring pixels of a specific point called seed point and add them to the region of interest if the distance between the seed point and its neighbor is with a specific threshold. The comparison is repeated until a specific threshold is reached. The region-growing algorithm was first explained by Adams and Bisch of in [11] where the algorithm was explained as follows: the region-growing algorithm starts by selecting a seed point, this seed expresses the initial region which is composed of one or more points and is represented by the set Ai, where i=1,2,...,n where n is the number of pixels in the initial selected region. let T be the neighbors set that represents all neighbors to at least one element in Ai (the initial defined region) and is represented by Eq. (4).

$$T = \left\{ x \notin \cup_{i=1}^{n} A_i : N(x) \cap \cup_{j=1}^{n} A_j \right\}. \quad (4)$$

In equation (4), N(x) represents the immediate neighbors of the pixel x. After defining the set T an examination step is done testing if the neighbors of each x belong to T, this step will be done one after another in turn. In the case that N(x) intersects region Aj, $\delta(x)$ a similarity difference between x and the intersecting region is calculated using Eq. (5).

$$\delta(x) = \left| g(x) - \text{mean}_{y \in A_j}\{g(y)\} \right|, \quad (5)$$

where g(x) is the grey level value of the point x and "mean" will be the average of all pixels y of the same grey level. In the case of intersecting N(x) with more than a region then Aj will be considered fulfilling $\delta(x)$ to the minimum. Repeatedly, each pixel x∈ T will have a value δ. The last step of the algorithm will be appending every pixel z in T that satisfies Eq. (6) to the region is alternative to $\delta(z)$, where $\delta(z)$ has the smallest similarity difference to pixel x that belongs to the set T.

$$\delta(z) = \min_{x \in T}\{\delta(x)\} \quad (6)$$

The new state of the region A_i is considered as the input for the new iteration. This process is repeated until all image pixels are examined.

2.3 FSPRG Method

In the proposed tumor segmentation technique, due to the similarities of the intensities of the liver tissues and the tumor the Fuzzy C-Means clustering technique has not been enough for complete accurate tumor segmentation from segmented liver 2D CT images. A supplementary method has been obligatory for accurate tumor extraction. In the proposed work, region growing has been chosen to accomplish the tumor extraction work after applying Fuzzy C-means algorithm as a primary step of the fuzzy seeded region-growing method.

Given an image of size 256x256 where the image represents a primary HCC infected image, the image is prepared to apply fuzzy C-means method on it by defining the number of clusters. By studying the histogram of the image in Fig. 2, it is shown that the intensities of the image are classified in to mainly 3 clusters. The first cluster represents approximately the background tissues, the second cluster represents approximately the tumor tissues and the last cluster represents approximately the liver tissues.

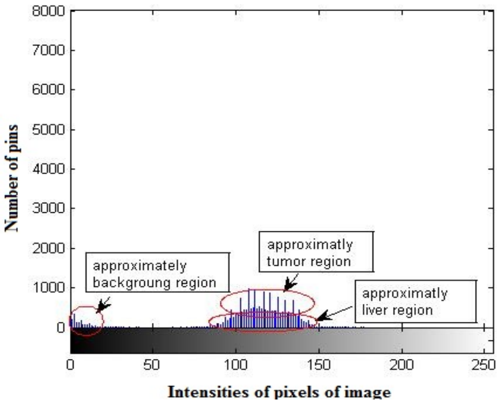

Fig. 2: Image Histogram.

After defining the number of clusters, the initial clusters' centers are chosen. Clusters centers are chosen approximately from the histogram. The first cluster is the background intensity region which is the regions of the image that almost have zero intensity, the second is the liver intensity region which is determined by the help of the seed point explained in [10] and the last cluster center is chosen randomly that should determine the tumor pixels region. The fuzzy c-means algorithm is applied to the image to divide it into three clusters as shown in Fig. 3 using the selected initial cluster's centers. The clusters region is presented by the bright pixels in the image. Fig. 3(a) represents the original image of the infected liver, Fig. 3(b) represents approximately the background likely pixels cluster, Fig. (c) represents approximately the tumor likely pixels cluster and Fig. (d) represents approximately the liver likely pixels cluster.

As shown in **Error! Reference source not found.**, the image that represents the likely tumors pixels is chosen to continue in the procedure, where some morphological operations which are image filling, image erosion and image filtering. All were applied to the selected image for enhancement as shown in **Error! Reference source not found.**5. After applying morphological operations the number of objects in the image is calculated.

The expected result is one of the following cases, the first case is that there is no object that is detected in the image so the liver is tumor free. The second case, there is only one object in the image which may indicate that there exists a lesion in the liver. The final case, there is more than one object in the image which may indicate that the liver contains more than one lesion. In the second and third cases there is further work to be done. In the case of only one object the center of the object is detected and used as an accurate seed point for the region-growing algorithm otherwise in the case of more than one object as shown in **Error! Reference source not found.**5(c) there may be FP (false positive) pixels detected. Another round of filtering is needed to be sure of the results and then the centers of all the objects is defined for accurate region growing for each object. In the case of the illustrated example after applying another round of morphological operations the false positive pixels where eliminated and the resulted image is given in Fig6. Fig.6: **Case study (1) after applying another round of morphological operations**.6: Case study (1) after applying another round of morphological operations, this illustrates that there is actually only one object that has been found and the center of that object is detected for accurate region-growing step as the results shown in Fig. 7. The results are enhanced and post processed by some morphological operations for the final results in Fig. 8 which represent the tumor in grey level.

(a) original image (b) first cluster

(c) second cluster (d) third cluster

Fig. 3: Case study (1) Three Clusters of the image.

After the tumor is segmented from the liver the area of the tumor is calculated from the binary image for further assessment of the tumor and size of the tumor with respect to the liver size that is calculated using the following formula in equation (7)

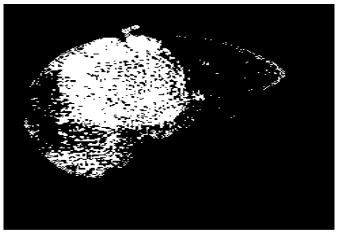

Fig. 4: Case study (1) representing the Tumor cluster.

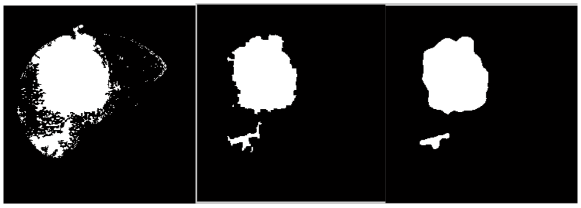

(a) (b) (c)

Fig. 5: Case study (1) after morphological operations.

Fig.6: Case study (1) after applying another round of morphological operations.

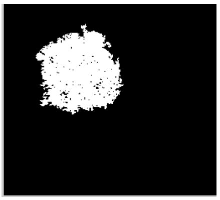

Fig. 7: Case study (1) after region growing.

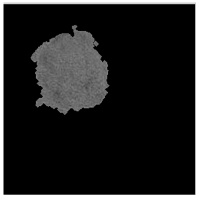

Fig. 8: Image of segmented Tumor.

2.4 Tumor Parameters and Safe Area

$$\text{Tumor size } \% = \frac{\text{area of segmented tumor}}{\text{total area of segmented liver}} * 100 \qquad (7)$$

For the purpose of computing the diameter of the tumor a laplacian of Gaussian (LOG) curve as a template mask is used to compare all the intensities in the image of the segmented liver. Followed by 2-D convolution that convolves the image with the template, this aims to find all the points which correspond to the template mask. Then, the maximum points that represent the point of edges are calculated and are plotted as shown in figure 9(a) where,

the edge of the segmented liver is well defined. The diameter of the tumor can be computed approximately by knowing the width and height of an ellipse drawn to the edges of the tumor as shown in figure 9 (b).

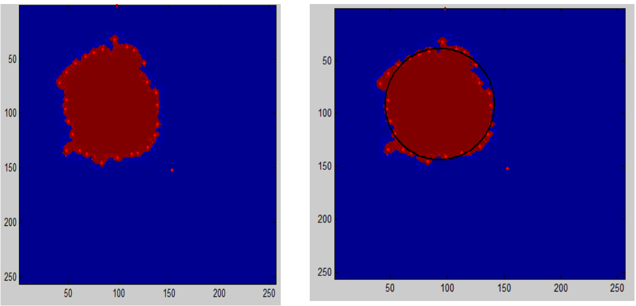

(a) (b)

Fig. 9: Segmented tumor detected edge.

One of the important measurements that is combined with the tumor assessment is the safe area which is the area that contains the neighboring cells of the tumor that have high probability to be affected by the tumor cells [19-21]. Estimating the safe area or the neighbor cells to the tumor cells plays an important role in reducing the spread of the tumor. In addition, knowing the safe area helps in further assessment of the texture of the area around the infected liver cells. To achieve tumor's safe area, as shown in figure 10 the same process has been applied using a smaller template mask to result in an image with three layers detected the first layer is the tumor layer, the second is the tumor edge layer and the third is the intermediate intensities between the liver pixels and the tumor pixels.

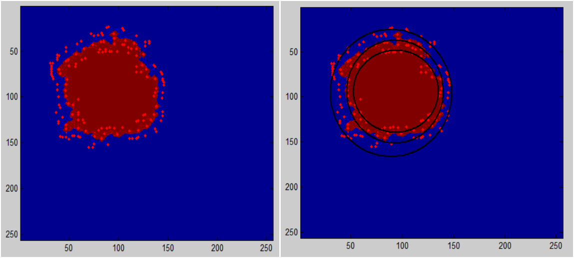

(a) (b)

Fig.10: Segmented tumor detected safe area.

3 Experimental Results

This subsection of the work is divided into three parts as follows: First, a brief explain of the data set is used in this work. Second, the results of the proposed work is discussed. This subsection ends up with a comparison of the proposed work with other related methods.

3.1 Data Set

In this proposed work we have used a testing data set of 14 CT of primary diagnosed HCC patients images. 10 images of the data set are taken from an online reference for infected liver imaging called liver imaging Atlas [18] and the other 4 2D CT images are taken from [13] and are used for testing and comparing the proposed algorithm. The format of all taken images is JPG and of size 256x256, where each image represents the extracted liver of one patient. The images are preprocessed to segment the liver from the whole 2D CT images by [10].

3.2 Results of Applying FSPRG Algorithm to the Dataset

This proposed work is coded using MATLAB R2013b on hp ProBook 4540s. Each image of the dataset is experimented for 10 times to be sure of the results. The data set is divided into two sets. The first set is 4 images of low contrast, where the liver pixels and the tumor pixels have very likely intensities as shown in Fig. 11. The second set is the set of images that are of high contrast, where there is a remarkable difference in intensities between the liver and the tumor as shown in Fig. 12. In Fig. 11 and Fig. 12, p1..p10 represents the 10 images of different patients. Results of the work are first compared to the results of the fuzzy c-means algorithm and the comparison is done with the two sets. The comparison of applying the FCM algorithm and FSPRG algorithm using the set of low contrast images is listed in Fig. 11 where, Fig. 11(a) represents the image of the segmented liver image. Fig. 12 (b) represents the image of the segmented tumors using only FCM. Figure 12(c) represents the results of the proposed algorithm FSPRG. The FCM algorithm alone has not been able to completely segment the tumor region from the liver while the FSPRG algorithm has succeeded to segment the tumor region from the liver.

The comparison with the set of 6 high contrast images is listed in Fig. 12. The proposed algorithm is also tested with a liver image that is pre-diagnosed with severe HCC as shown in Fig. 12 case P10. The liver contains more than one tumor in different areas. The proposed method has succeeded to segment the tumors accurately as shown in Fig. 12(c).The quality metrics of images approximation are calculated for the 10 images, where two values are concluded. First, the peak signal-to-noise ratio, PSNR , where the graph in Fig. 13 shows that the proposed FSPRG algorithm has higher PSNR than the FCM algorithm compared to the original manual extracted tumors. Second, the mean square error, MSE, where the proposed algorithm FSPRG has lower MSE than FCM algorithm.

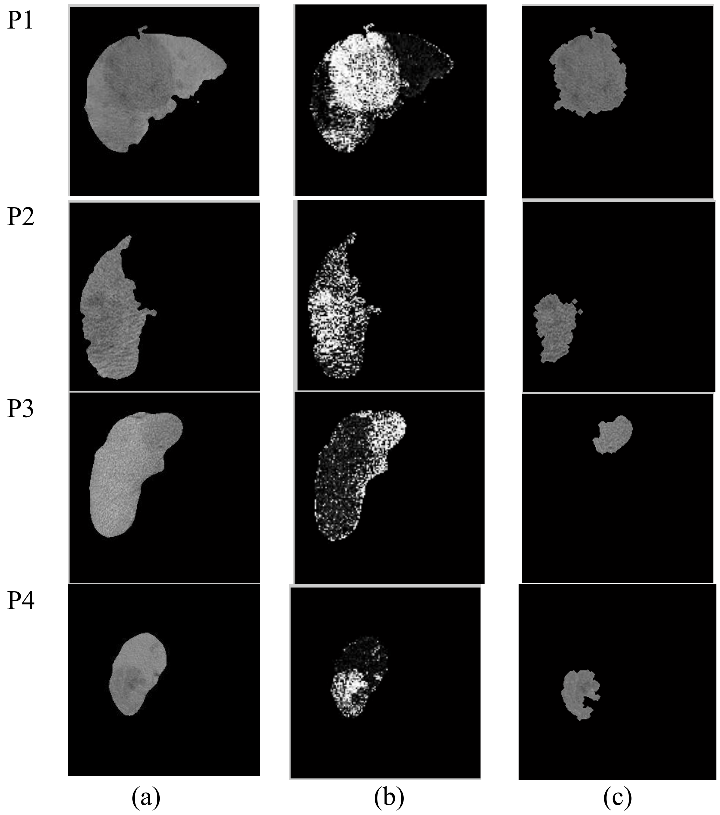

Fig. 11: Four different patient case studies with high image contrast.

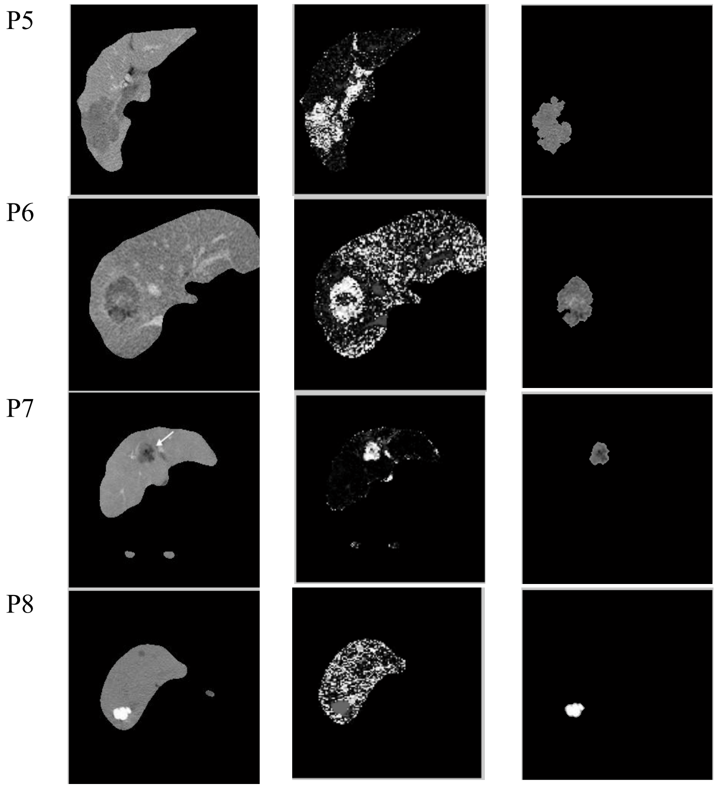

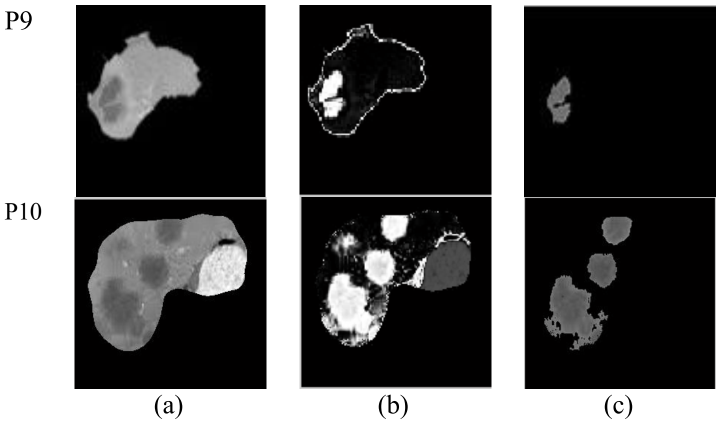

Fig. 12: Six different patient case studies with low image contrast.

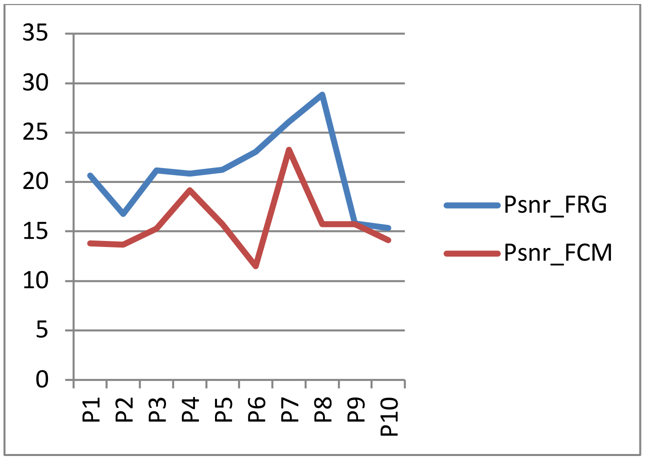

Fig. 13: peak signal-to-noise ratio, PSNR.

The results are also compared with the work done in [13], where KFCM (kernel fuzzy C-means) is introduced to segment and measure the tumor area from segmented liver. The comparison is done on images proposed by [13] and the results of the comparison are shown in **Error! Reference source not found.**15. The comparison shows that the KFCM algorithm segmented a noisy tumor area as shown in **Error! Reference source not found.**15(c) compared to the results of the proposed FSPRG algorithm that shows its effectiveness for tumor segmentation in **Error! Reference source not found.**15(b) while **Error! Reference source not found.**15(a) shows the images of the segmented liver that are used in the comparison. The quality metrics of images approximation are calculated for the 4 images, and the results are shown in **Error! Reference source not found.**. The graph shows that the proposed algorithm FSPRG has higher PSNR and similarly lower MSE than KFCM.

3 Tumor Parameter Results

The incoming figures show the effectiveness of the proposed FSPRG method in calculating tumor diameter and safe area. Figures 18 to 20 show obtained result. The tumor classification stages of case study P1 is illustrated in Fig. 18 where, Fig. 18(a) represents the segmented liver image, Fig. 18(b) represents the image of the segmented tumor, Fig. 18(c) represents the calculated height and width of the tumor. Fig. 18(d) represents the three RIO (inside tumor region, border tumor region and safe area tumor region) and the calculated height and width of safe area.

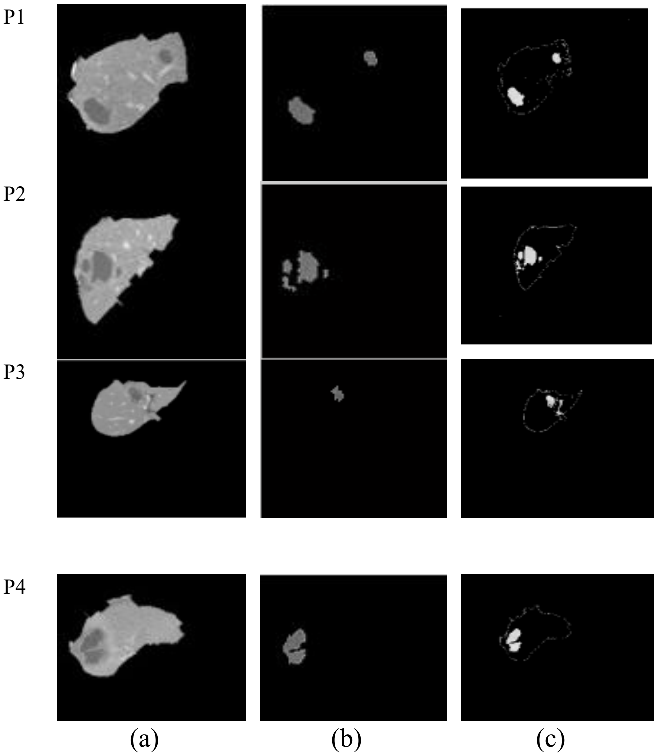

Fig.15: Four test cases for comparing FSPRG and KFCM.

On the same way the case study illustrated in Fig. 19 where, Fig. 19(a) represents the segmented image, figure 19(b) represents the segmented tumor, Fig.19(c) represents the tumor height and width while, Fig. 19(d) represents the safe area dimensions.

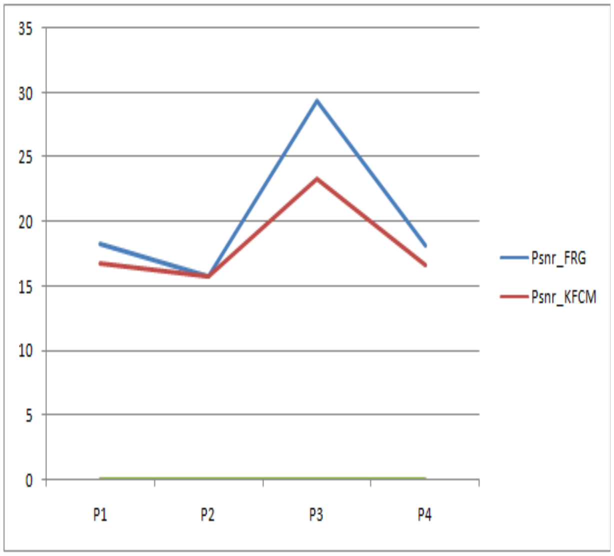

Fig. 16: peak signal-to-noise ratio, PSNR.

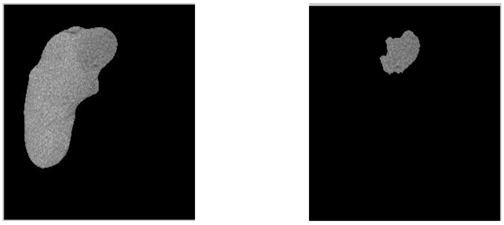

(a)segmented liver (b) segmented tumor

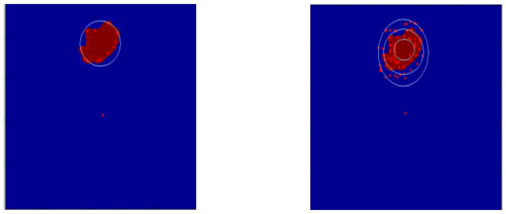

(c) tumor
width(~3.4cm)
height(~1.3cm)

(d) safe are
width(~0.8cm)
Hegth(~0.5cm)

Fig.18: (Case study 1):Tumor classification stages.

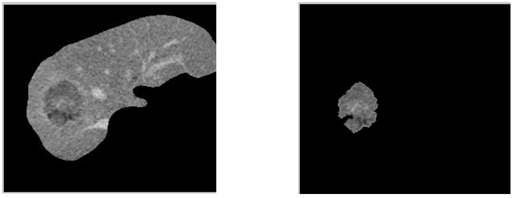

(a)segmented liver (b)segmented tumor

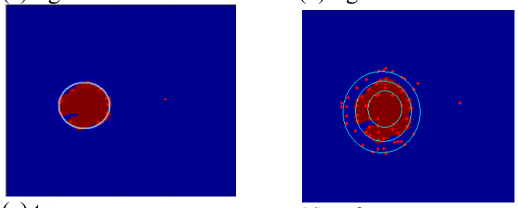

(c) tumor
Width(~2.8cm)
Height(~1.5cm)

(d) safe area
Width(~1cm)
Height(~0.6cm)

Fig.19: **(**Case study 2): Tumor classification stages.

Another case study is explained in Fig. 20. Fig. 20(a) represents the segmented liver, figure 20(b) represents the segmented tumor, 20(c) represents the computed dimensions of the tumor and in figure 20(d) represents the dimensions of the safe area and the three detected regions.

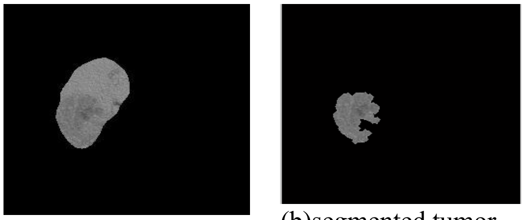

(a)segmented liver (b)segmented tumor

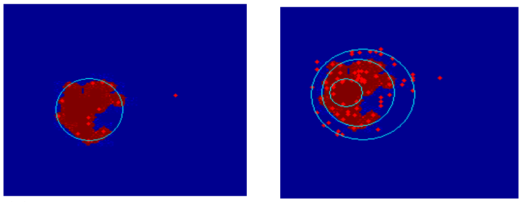

(c) tumor
Width(~3cm)
Height(~1.4cm)

(d) safe area
Width(~1.2cm)
Height(~0.5cm)

Fig. 20: (Case study 3): Tumor classification stages.

A comparison was done between the dimensions of the tumor resulted by FSPRG and the dimensions of the tumor computed manually and the results was as follows:

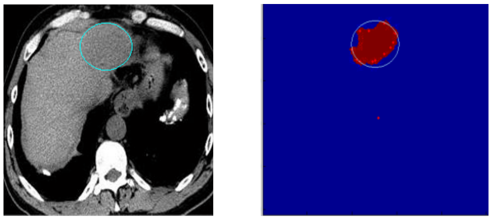

(a)
Original Tumor
width(~3.5cm)
height(~1.4cm)

(b)
FSPRG tumor
width(~3.4cm)
height(~1.3cm)

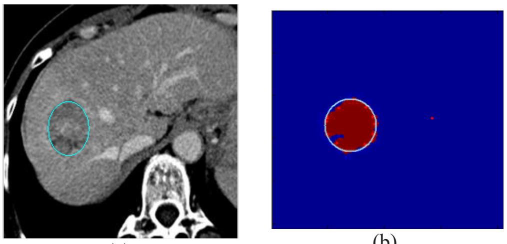

(a)
Original Tumor
Width(~2.9cm)
Height(~1.6cm)

(b)
FSPRG tumor
Width(~2.8cm)
Height(~1.5cm)

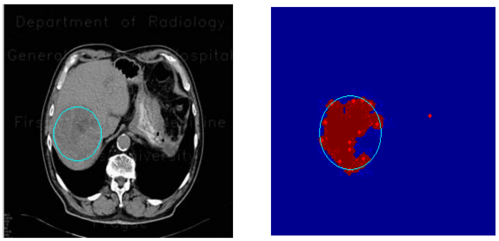

(a)
Original Tumor
Width(~3cm)
Height(~1.5cm)

(b)
FSPRG tumor
Width(~3cm)
Height(~1.4cm)

Fig. 21: comparison between original tumor dimentions and FSPRG tumor dimension.

The comparison in figure 20 shows three case studies for comparing manual and FSPRG computed tumor dimensions. Also the whole data set entered the comparison and the results have shown that our proposed method has succeeded to compute the segmented tumor dimensions approximately compared to manual dimensions by 98%.

4 Perspectives

The accuracy of the tumor segmentation from image of segmented image plays an important role in accurate diagnosis of the disease. In this paper we have proposed an integrated hybrid FSPRG algorithm that accurately segments tumors from the liver to be able to calculate the tumor dimensions together with defining the safe area. The experimental results show that our approach is adequate and achieves high accuracy in segmenting the tumors from the liver when compared with the segmentation results of FCM and KFCM especially in case studies with poor intensities or high noise densities. The average PSNR has been improved from 15.81064 to 20.97258 and the MSE has been reduced in an inversely proportional manner from 2.08E+03 to 7.64E+02. In addition, the results of comparing the manually-detected tumor dimensions (height and width) are compared to the tumor dimensions resulting from the proposed FSPRG. Results show that this automatic method achieves accurate dimensions for 98% of the case studied. For future work, the ROIs detected in the stage of contouring the safe area will be used for texture analysis for the purpose of tumor classification either malignant or benign.

References

[1] Luo, S., Li, X., & Li, J. Review on the methods of automatic liver segmentation from abdominal images. Journal of Computer and Communications., **2(02)**, 1,2014.

[2] Feng, Y., Guo, H., Zhang, H., Li, C., Sun, L., Mutic, S., ... & Hu, Y. A modified fuzzy C-means method for segmenting MR images using non-local information. Technology and Health Care., **24(s2)**, S785-S793,2016.

[3] Bezdek, J. C., Ehrlich, R., & Full, W. FCM: The fuzzy c-means clustering algorithm. Computers & Geosciences., **10(2-3)**, 191-203,1984.

[4] Li, B. N., Chui, C. K., Chang, S., & Ong, S. H. Integrating spatial fuzzy clustering with level set methods for automated medical image segmentation. Computers in biology and medicine., **41(1)**, 1-10,2011.

[5] Mekhmoukh, A., & Mokrani, K. Improved Fuzzy C-Means based Particle Swarm Optimization (PSO) initialization and outlier rejection with level set methods for MR brain image segmentation. Computer methods and programs in biomedicine., **122(2)**, 266-281,2015.

[6] Yugander, P., & Reddy, G. R., May. Liver tumor segmentation in noisy CT images using distance regularized level set evolution based on fuzzy C-means clustering. In Recent Trends in Electronics, Information & Communication Technology (RTEICT), 2017 2nd IEEE International Conference on., 1530-1534, IEEE,2017.

[7] Moghbel, M., Mashohor, S., Mahmud, R., & Saripan, M. I. B. Automatic liver tumor segmentation on computed tomography for patient treatment planning and monitoring. EXCLI journal., **15**, 406, 2016.

[8] Mary, J. M. Image Segmentation Technique-A study on Region Growing Approaches,2017.

[9] Zhao, B., Schwartz, L. H., Jiang, L., Colville, J., Moskowitz, C., Wang, L., ... & Kalaigian, J. Shape-

constraint region growing for delineation of hepatic metastases on contrast-enhanced computed tomograph scans. Investigative radiology., **41(10)**, 753-762, 2006.

[10] Elmorsy, S. A., Abdou, M. A., Hassan, Y. F., & Elsayed, A., March. K3. A region growing liver segmentation method with advanced morphological enhancement. In 2015 32nd National Radio Science Conference (NRSC) ., 418-425, IEEE, 2015.

[11] Adams, R., & Bischof, L. Seeded region growing. IEEE Transactions on pattern analysis and machine intelligence, 16(6), 641-647,1994.

[12] Tapper, E. B., & Lok, A. S. F. Use of liver imaging and biopsy in clinical practice. New England Journal of Medicine., **377(8)**, 756-768, 2017.

[13]Das, A., & Sabut, S. K. Kernelized fuzzy C-means clustering with adaptive thresholding for segmenting liver tumors. Procedia Computer Science., **92**, 389-395,2016.

[14] Zaitoun, N. M., & Aqel, M. J. Survey on image segmentation techniques. Procedia Computer Science., **65**, 797-806, 2015.

[15] Lee, L. K. Region-growing based segmentation and bag of features classification for breast ultrasound images(Doctoral dissertation, Universiti Malaysia Pahang), 2017.

[16] Puritat, K., Chernbumroong, S., & Sureephong, P. A region growing based segmentation for recognition system method implement with coin based application. International Journal of Applied Engineering Research., **12(6)**, 950-955, 2017.

[17] Tan, S., Li, L., Choi, W., Kang, M. K., D D'Souza, W., & Lu, W. Adaptive region-growing with maximum curvature strategy for tumor segmentation in 18F-FDG PET. Physics in Medicine & Biology., **62(13)**, 5383, 2017.

[18] https://www.liveratlas.org.

[19] Wagstaff, L., Kolahgar, G., & Piddini, E. Competitive cell interactions in cancer: a cellular tug of war. Trends in cell biology., **23(4)**, 160-167, 2013.

[20] Di Gregorio, A., Bowling, S., & Rodriguez, T. A. Cell competition and its role in the regulation of cell fitness from development to cancer. Developmental Cell., **38(6)**, 621-634, 2016.

[21] Loaiza, N., & Demaria, M. Cellular senescence and tumor promotion: is aging the key?. Biochimica et Biophysica Acta (BBA)-Reviews on Cancer. **1865(2)**, 155-167,2016.

[22] M. Hagan, H. Demuth, M. Beale, Neural Network Design, PWS publishing Company: Boston, MA, USA, 1996

[23] M. Zidan, A.-H. Abdel-Aty, M. El-shafei, M. Feraig, Y. Al-Sbou, H. Eleuch and M. Abdel-Aty, Quantum Classification Algorithm Based on Competitive Learning Neural Network and Entanglement Measure, Appl. Sci., **9(7)**, 1277, 2019.

[24] Y. Huang, Advances in Artificial Neural Networks Methodological Development and Application. Algorithms, **2**, 973–1007, 2009.

[25] A. Sagheer, M. Zidan and M. M. Abdelsamea, A Novel Autonomous Perceptron Model for Pattern Classification Applications, Entropy, ***21(8)***, 763, 2019.

Shaimaa Aly Elmorsy is an assistant lecturer of computer science, working in both research and teaching. She is currently an assistant lecturer and a Ph.D. student in Mathematics and Computer science department, Faculty of science, Alexandria university. She has some international publications. Her researches vary between image processing and artificial intelligence

Mohamed AbdelRahman Abdou is an associate professor of communications and computer systems engineering, working in both research and teaching for more than 20 years. He is currently an associate professor in Informatics Research Institute, City for Scientific Research & Technology Applications. He has a distinguished international publications record. He has a great experience in establishing new universities and research centers. He is also an adjunct professor at Pharos University in Alexandria, acting the Head of Electrical Engineering Department.

Yasser Fouad Mahmoud Hassan, Professor of Computer Science at Faculty of Science- Alexandria University. Dean of Faculty of Computers Science and AI- Pharos University BSc. (Bachelor of Science): Computer Science from Faculty of Science – Alexandria University .PhD. In Computer Science from Toin University of Yokohama-Japan .

Ashraf Elsayed, received B.Sc. degree from the Alexandria University, Alexandria, Egypt, in 1995, the M.Sc. degree from the Alexandria University, Alexandria, Egypt, in 2004, both in Computer science. And the Ph.D. degree from the University of Liverpool, UK, in 2012, in Computer science. His currently position: Assistant Professor at University of Science and Technology, Zewail city of Science and Technology, Giza, Egypt. (On leave as Assistant Professor at Faculty of Science - Alexandria university, Alexandria, Egypt).His research interests include Data Science - Big data Analytics - Deep learning – Quantum machine learning.